



SYNTHESIS, CHARACTERIZATION, AND BIOLOGICAL EVALUATION OF 3-BROMO ISOQUINOLINE DERIVATIVES: POTENTIAL LEAD MOLECULES FOR ANALGESIC AND ANTI- INFLAMMATORY AGENTS

Tariq Javed¹, Hashmat Ullah^{2*}, Sheikh Abdur Rashid^{3*}, Muhammad Tariq Khan⁴, Nadia Shamshad Malik⁵, Ahmed Sadiq Sheikh⁶, Nitasha Gohar⁷, Ayesha Rashid⁸, Amina Riaz⁹, Muhammad Atta ur Rehman¹⁰

^{1,2*,3*}Gomal Centre of Pharmaceutical Sciences, Faculty of Pharmacy, Gomal University, D. I. Khan.29111 Pakistan

^{4,5} Faculty of Pharmacy, Capital University of Science and Technology, Islamabad, 44000 Pakistan

⁶ Faculty of Pharmacy, My University, Islamabad, 44000 Pakistan

⁷ Faculty of Pharmacy, Capital University of Science and Technology, Islamabad, 44000 Pakistan

^{8,9} Department of Pharmacy, The Women University Multan, 61000, Pakistan

¹⁰ Institute of Chemical Sciences, Gomal University, D. I. Khan.29111, Pakistan

***Corresponding Author:** Hashmat Ullah, Sheikh Abdur Rashid

*Gomal Centre of Pharmaceutical Sciences, Faculty of Pharmacy, Gomal University, D. I.

Khan.29111 Pakistan, Email: drhashmat28@gmail.com , sheikhabdurrashid11@gmail.com

Abstract:

Nitrogen containing heterocycles have gained massive research attention since they are frequently found as naturally occurring bioactive compounds. This status of N-heterocycles makes it dynamic to design methods to expand their synthetic efficacies and review the effects of their modifications on biological systems. In the present study we synthesized several 3-bromo isoquinoline derivatives which are nitrogen-containing arylated heterocycles via Suzuki coupling reaction. The prepared compounds were physically and chemically characterized by Fourier transform infrared (FTIR), ¹H NMR, and ¹³C NMR spectral data. Biological screening such as antibacterial, antifungal, antioxidant, analgesic, and anti-inflammatory, COX2 inhibitor activities along with toxicity concerns were checked. Molecular docking studies were performed to confirm the ligand protein binding and type of binding interactions resulting in the biological activities of the compounds. Therefore, our study proposed that the 3-bromo isoquinoline derivatives hold noteworthy analgesic and anti-inflammatory activity and have very positive toxicity values. These facts serve as basis that keeping the activity and safety considerations these molecules might attend researcher's attention as a lead molecule for the discovery of potent analgesic and anti-inflammatory agents.

Keywords: N-heterocycles, bioactive compounds, 3-bromo isoquinoline derivatives, Suzuki coupling reaction, analgesic activity, and anti-inflammatory activity.

1. Introduction

Bioactive molecules are created through chemical synthesis and development to become marketable pharmaceutical agents that can be purchased. The most significant organic compounds, heterocyclic compounds, are frequently found in molecules of interest in medicinal chemistry [1]. Since they are prevalent in nature and can be found as subunits in a variety of natural products, including vitamins, hormones, and antibiotics, nitrogen-containing heterocycles are particularly significant to the study of life. Several representative alkaloids and other naturally occurring nitrogen-containing substances, displaying a range of biological activities [2] and several of them are even prescribed drugs such as serotonin, [3] thiamine, which is also called water soluble vitamin B1 [4], atropine [5] narcotics morphine [6], and codeine, (activity enhances when it is sandwich with paracetamol (acetaminophen) or a nonsteroidal anti-inflammatory drug (NSAID) such as aspirin (acetyl salicylic acid) or ibuprofen [7], papaverine [8], coniine [9], caffeine [10] and nicotine [11].

One of the most useful cross-coupling reactions between aryl or vinyl boronic acid and aryl or vinyl halides as well as with various reagents like alkenes, alkynes, amines, pseudohalides, metallorganic compounds, etc. is the Suzuki- Miyaura reaction, also known as the "Suzuki coupling reaction," which is currently being catalysed by palladium (0) complexes. Suzuki cross coupling reactions with palladium as the catalyst are one of the most potent and versatile ways to create C—C bonds [12]. Since its discovery by Suzuki and Miyaura in 1979, the Suzuki-Miyaura cross-coupling reaction has primarily been used in laboratories and industries to create aliphatic and aromatic C-C bonds by coupling an organoboron reagent with an organic halide in the presence of a palladium or nickel catalyst and a base [13].

Isoquinoline (ISOQ), also known as benzopyridines, is a heterocyclic aromatic chemical molecule containing nitrogen that is made up of a benzene ring fused to a pyridine ring. One of the most significant isoquinoline derivatives in our research i.e., 3-bromo isoquinoline is used as lead compound to prepare multiple N-arylated derivatives. The chemical formula is C₉H₆BrN with a molar mass of 208.06 g/mol.

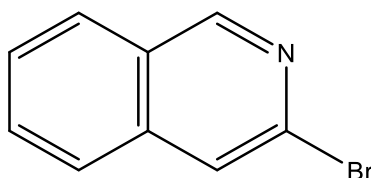


Figure 1: Structure of 3-bromo isoquinoline

According to FDA databases, N-based heterocycles are present in about 60% of novel small-molecule drugs, demonstrating their structural importance in drug development and drug discovery [14]. The stability and effectiveness of N-heterocycles in the human body as well as the ease with which the nitrogen atoms can form hydrogen bonds with DNA explain why they are so common in biologically active compounds. In reality, N-based heterocycles agents' anti-cancer effects are primarily a result of their inclination to interact with DNA via hydrogen bonding [15].

ISOQ and its derivatives are present in many natural products and are thought to be pharmacologically active due to their capacity to express a wide range of biological activities, such as those that are anti-malarial, anti-HIV, anti-tubercular, anti-tumor, anti-fungal, anti-glaucoma, anti-Parkinson's disease, etc [16],[17]. Insecticides, dyes, and paints are all produced using them [18]. They serve as a solvent for the extraction of resin and terpenes [19].

Due to its antibacterial [20], analgesic [21], anti-inflammatory [22], and anticancer activity, isoquinoline derivatives have attracted attention in the quest for novel pharmacologically active drugs, 3-bromo isoquinoline, a synthetic isoquinoline compound, has some specific molecular targets and modes of action that approve this chemical for further study as a potential anti-inflammatory and analgesic action in the future.

Nitrogen heterocyclic compounds like 3-bromoisoquinoline have always been desirable targets for synthetic organic chemists because they exhibit a variety of biological activities. Since many of them are present in natural products, particularly alkaloids, they have drawn a lot of attention from the synthetic community, particularly from those working on total synthesis of natural products [23]. The vast majority of nitrogen heterocyclic compounds have thus been the subject of ongoing investigations from various angles and have thus found applications in pharmaceutical research and drug discovery [24, 25]. Due to their wide range of biological activities and numerous applications in the vast field of pharmacy, nitrogen-containing heterocycles are currently attracting the attention of medicinal chemists and biologists [26-28].

In last decade, analysis showed the importance of the nitrogen based heterocyclic compounds in the field of medicine [29]. This analysis showed that indeed about 60% of small-molecule drugs contain an N-based heterocycles as common architectural cores [30]. Recent advances in nitrogen-based heterocyclic compounds resulted in a useful biological activities such as anticancer chemotherapy [31], antioxidant [32], analgesic [33], antipyretic [34] antimicrobial [35], and anti-inflammatory activities [2, 36].

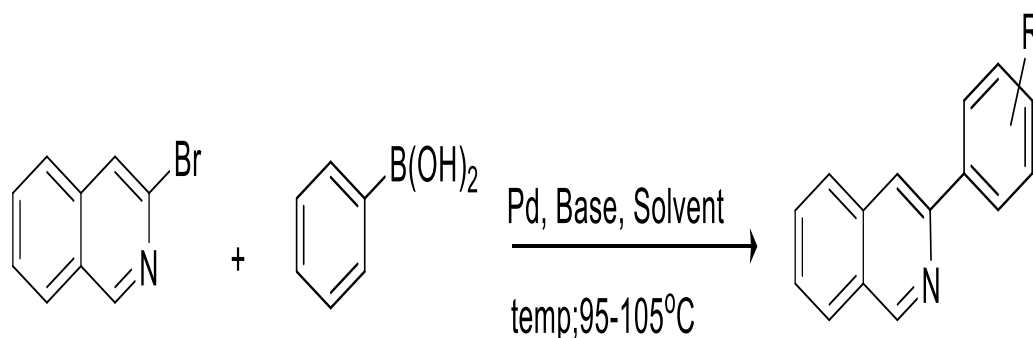
1.1. Study Rationale

It has been observed from the literature that nitrogen is strangely common in many anti-inflammatory and analgesic drugs; therefore, nitrogen-containing heterocycles are being explored widely. Interestingly, the introduction of nitrogen atom in the cyclic systems along with arylation, amended the therapeutic potential. As C-C linkages are considered as arylated compounds, the present study was designed to synthesize structural substitution of 3-bromo isoquinoline and different arylated boronic acids to explore their anti-inflammatory and analgesic potential. Since many of the existing anti-inflammatory and analgesics have lost their efficacy due to potential gastric irritation and severe side effects, our aim in the present study was to develop anti-inflammatory and analgesic lead molecules that can also target these side effects. Keeping in view the above-mentioned facts and search for new potent anti-inflammatory and analgesic candidates, the present study was designed to synthesize new hybrid molecules containing 3-bromo isoquinoline linked with different aryl through C-C linkage and heterocyclic nitrogen containing compounds and evaluate them for in vitro and in vivo anti-inflammatory and analgesic potential and in silico mechanistic investigation.

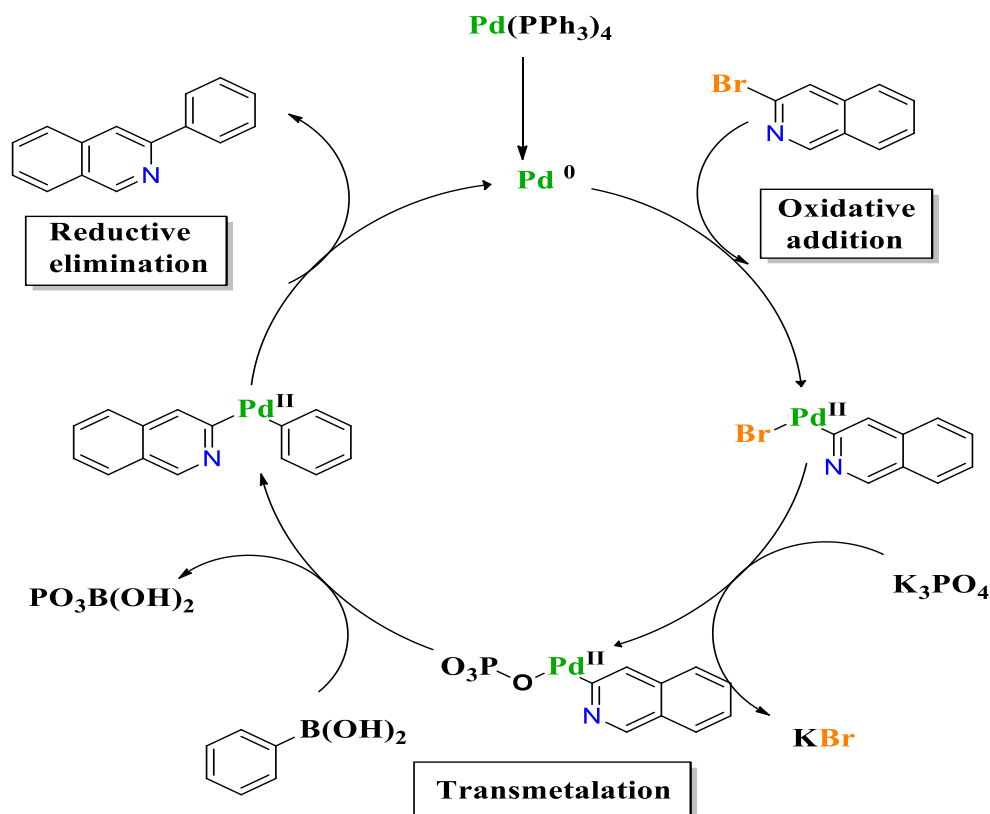
2. Results and Discussion

2.1. General Scheme of Synthesis

The Suzuki coupling reaction is generally carried out by reacting aryl 3-Bromo isoquinoline with aryl boronic acid under SMC conditions. Scheme 1 illustrates the general Scheme for the Synthesis of arylated heterocyclic compounds whereas scheme 2 illustrates the general mechanism of Suzuki coupling reaction for the Synthesis of arylated heterocyclic compounds.



Scheme 1. General Scheme for the Synthesis of arylated heterocyclic compounds



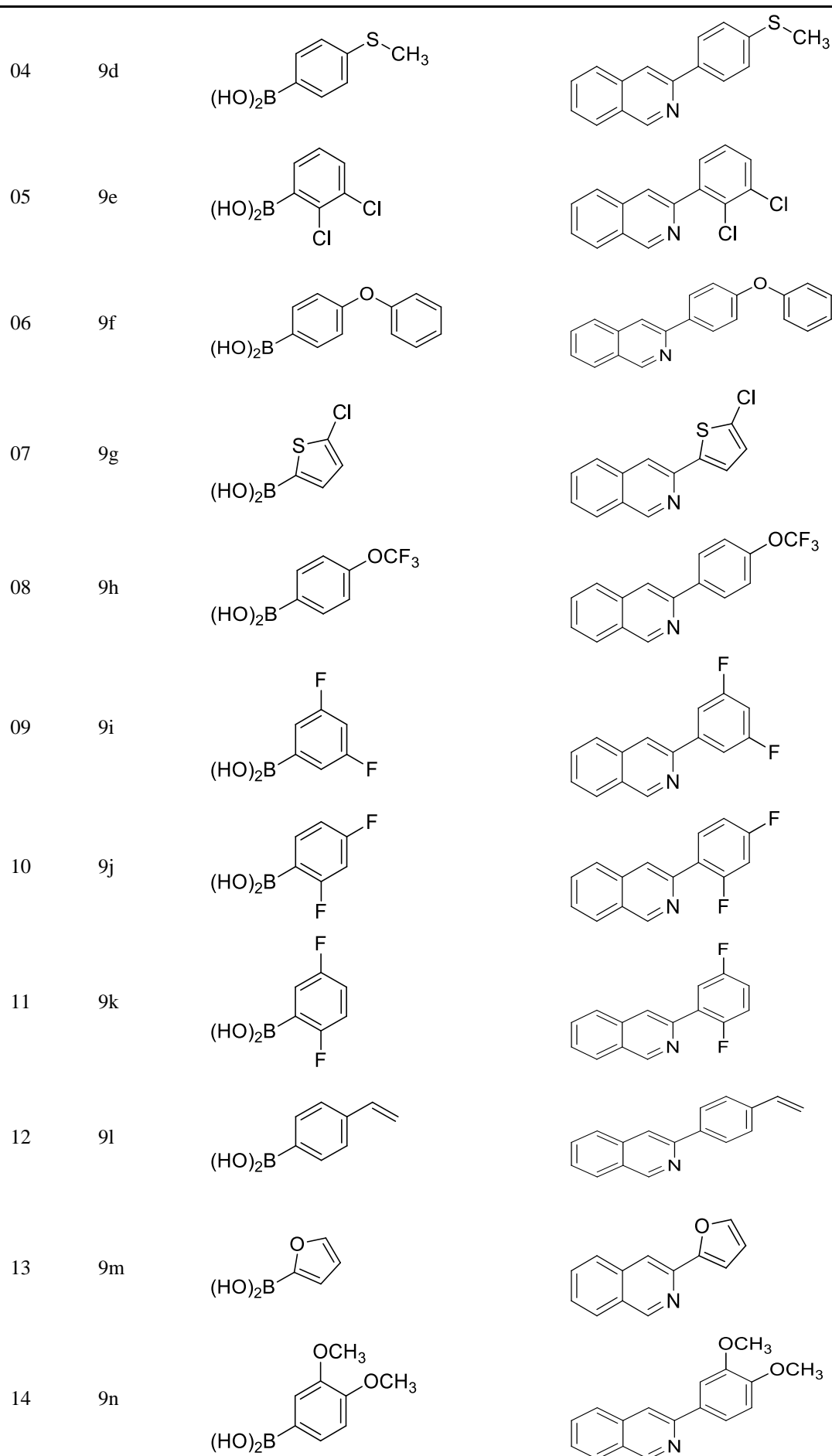
Scheme 2. General mechanism of Suzuki coupling reaction for the Synthesis of arylated heterocyclic compounds

2.2 Synthesis of N-containing 3-bromoisoquinoline derivatives.

In the present work, 3-bromoisoquinoline was reacted with various boronic acids to yield N-containing heterocyclic compounds via C-C linkage as a key intermediate [37] in the first step, which in turn was treated with a series of different arylated boronic acids (a-t), leading to the formation of N-containing heterocyclic compounds 9(a-t), as shown in scheme 1. The structural details of the newly synthesized 3-bromoisoquinoline derivatives are presented in Table 1. The physical parameters of the synthesized compounds, including melting point, physical form, percentage (% age) yield, along with molecular formula and molecular weights, were determined and are given in Table 2.

Table 1. Synthesized arylated heterocyclic compounds 9(a-t).

Sr #	Code	Boronic acids	Product
01	9a		
02	9b		
03	9c		



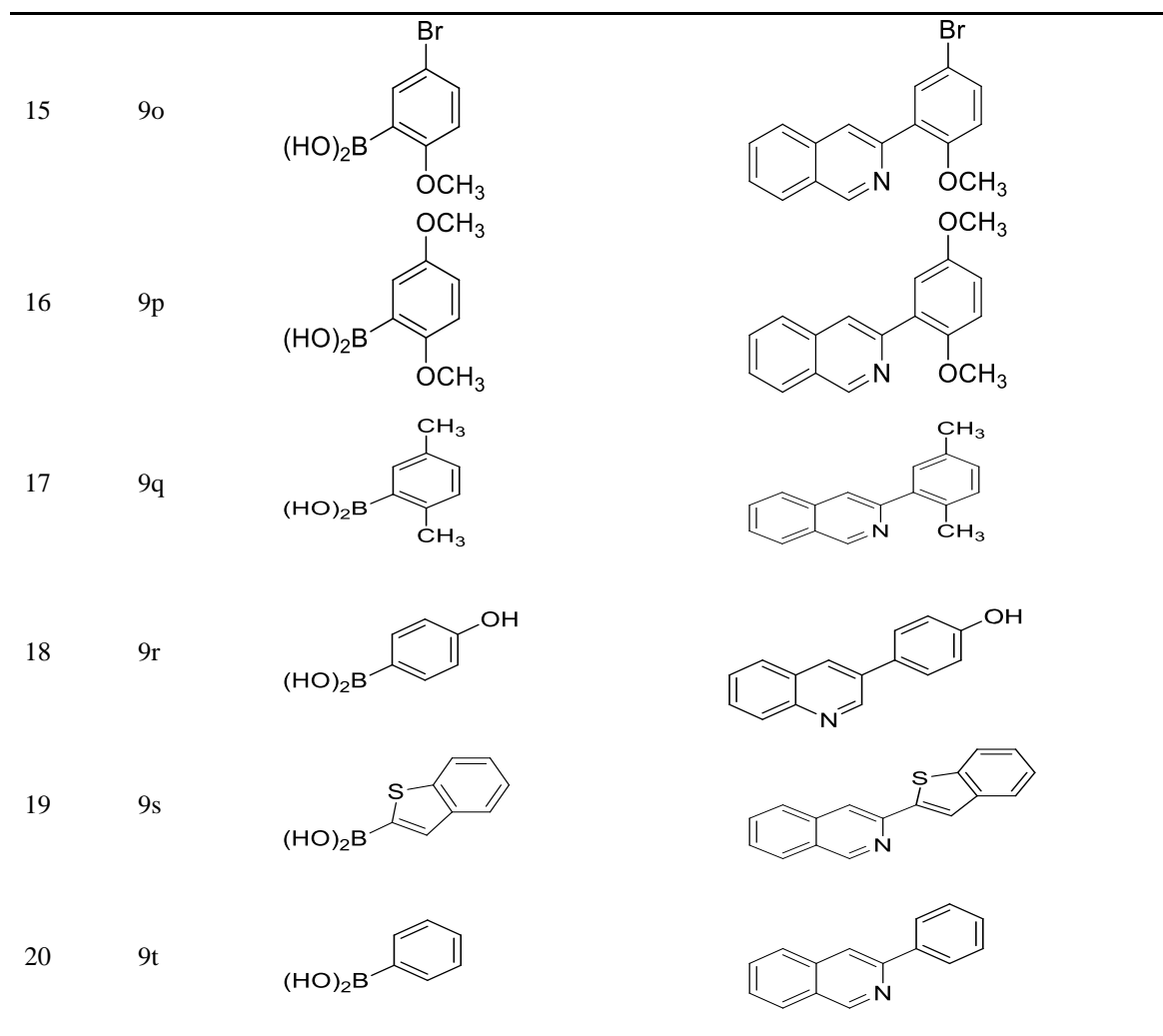


Table 2. Physical Data of the Synthesized Compounds (9a–t)

compounds	mol. formula	mol. weight (g)	mp (°C)	physical form	% yield	Rf value
9a	C17H13NO	247.29	239.75	solid	78	0.75
9b	C17H9F6N	341.25	210.52	solid	71	0.69
9c	C16H12FN	237.27	191.66	solid	81	0.81
9d	C18H13NS	251.35	212.95	solid	77	0.78
9e	C15H9Cl2N	274.14	239.64	solid	75	0.68
9f	C21H15NO	297.35	283.55	solid	67	0.71
9g	C13H8ClNS	245.73	260.87	solid	69	0.73
9h	C16H10F3NO	289.25	204.97	solid	69	0.69
9i	C15H9F2N	241.24	260.89	solid	83	0.84
9j	C15H9F2N	241.24	180.98	solid	82	0.81
9k	C15H9F2N	241.24	261.18	solid	81	0.82
9l	C17H13N	231.29	188.06	solid	76	0.76
9m	C13H9NO	195.22	161.45	solid	71	0.72
9n	C17H15NO2	265.31	246.8	solid	68	0.67
9o	C16H12BrNO	314.18	273.1	solid	68	0.75
9p	C17H15NO2	265.31	243.6	solid	74	0.81
9q	C17H15NO	233.31	202.34	solid	76	0.79
9r	C15H11NO	221.25	266.48	solid	81	0.66
9s	C17H11NS	261.34	308.73	solid	83	0.68
9t	C15H11N	205.25	154.76	solid	85	0.71

^a (N-Hexane/Ethyl acetate, 2:3), (HF-254)- silica

2.3. Characterization of newly synthesized derivatives

All the compounds were obtained as solids with sharp melting points. The progress of each reaction was monitored by TLC and the structural characterization was done by Fourier transform infrared (FTIR), ¹H NMR, ¹³C NMR and UV spectral data. FTIR spectra showed prominent peaks for C=C stretching at 1620-1680 cm⁻¹, C-C stretching at 1450-1550 cm⁻¹ confirming the formation of the desired compounds. Other important peaks included Ar-H stretching at 3020-3100 cm⁻¹, C-X stretching's in the range of 718-810 cm⁻¹, C=O stretching at 1680- 1750 cm⁻¹, O-H and stretching at 3300- 3600 cm⁻¹ peaks at higher frequencies in all compounds. In the ¹H NMR spectra of the synthesized compounds, all the protons resonated in their respective regions. The characteristic singlet peak of the linker CH₃ was observed in the region 1.3-2.0 ppm, while aromatic protons of aromatic moiety resonated as multiples at 7.25-7.87 ppm.

In the case of the N-containing heterocyclic compound 9a, one singlet peak for 3 protons at 2.2-2.8ppm were observed, while aromatic protons appeared in the expected region. In the case of 9b, aromatic ring protons resonated at 7.2-8.9 ppm. Similarly, for the 9c compounds, a doublet peak for methyl protons was observed at 1.2-1.8ppm downfield and aromatic ring protons resonated at 7.2-8.9 ppm. For the 9h compounds, aromatic protons of aromatic moiety resonated at 7.25-8.9 ppm. For the 9q compounds, one singlet peak for 6 protons at 1.2-1.8ppm were observed and aromatic protons of aromatic moiety resonated at 7.25-8.9 ppm. ¹³C NMR was also performed, which further confirmed the synthesis of the target compounds 9(a-t). The characteristic peak of the methyl moiety was noticed at 25-45 ppm in all methyl containing compounds. In addition, some characteristic peaks were observed in the aromatic range of 121 ppm to 166 ppm, while carbonyl carbon resonated downfield at 166- 180 ppm in C=O containing compounds.

2.4. Molecular Docking Analysis

Employing molecular docking, the existing affinity between ligands and protein targets was evaluated. AutoDock Vina [38] program was used for the docking analysis through PyRx [39] user interface. E-value (kcal/mol) was used to assess the affinity of protein and best docked pose complex. It provided prediction of binding free energy and binding constant for docked ligands. Binding affinities of ligands for COX-2 (PDB ID: 5KIR) and TNF- α (PDB ID: 2AZ5) can be seen in table 3.

For the investigation of the interactions based on binding of synthesised products in the protein active site, the synthesised compounds were docked to COX-2 binding site (PDB ID: 5KIR) and TNF- α binding site (PDB ID: 2AZ5). COX-2 and TNF- α are chosen for molecular docking studies because of their important roles in inflammation and the immune system, making them relevant targets for the creation of new treatments. Understanding these interactions can provide insights into the origins of sickness and aid in the development of therapeutic strategies. Furthermore, accurate ligand binding prediction is possible by virtue of the availability of their structural data. The standard was Celecoxib. The binding affinities of the produced compounds were evaluated and compared to Celecoxib, a common ligand.

The active site affinities of all the compounds are moderate to good. For COX-2 protein (PDB ID: 5-KIR), among all newly synthesized compounds, compound 9a, 9b and 9c exhibited the highest binding affinity of -8.7 each whereas 9l and 9q have exhibited binding affinity of -8.3, and -7.4 respectively. These compounds have shown significant Vander Waal, conventional hydrogen bond, Pi Pi T-shaped, Pi-Alkyl and Amide Pi stacked type interactions. The binding affinity of the reference standard celecoxib was -9.3. For TNF- α binding site (PDB ID: 2AZ5), among all newly synthesized compounds, compound 9b, 9c, 9h, 9p and 9q exhibited the highest binding affinity of -8.8, -9.4, -9.1, -8.2, and -8.5 respectively.

These compounds have shown significant Vander Waal, conventional hydrogen bond, carbo hydrogen bond, Pi Pi T-shaped, Pi-Alkyl and Amide Pi stacked type interactions. The binding affinity of the reference standard celecoxib was -7.8. Figure 2 to 6 depicts the binding interactions of protein 9a.9b.9c.9i, and 9q with the amino acid residues of COX-2's binding site in 2D (A) and

3D (B) images (PDB ID: 5KIR) respectively. Figure 7 to 11 depicts binding interactions of 9b,9c,9h,9p, and 9q with the TNF- α binding site's amino acid residues in 2D(A) and 3D(B) space (PDB ID: 2AZ5) respectively.

Table 3. Binding affinities of ligands for COX-2 (PDB ID: 5KIR) and TNF- α (PDB ID: 2AZ5)

Compound	COX-2 (PDB ID: 5KIR)	TNF- α (PDB ID: 2AZ5)
9a	-8.7	-7.7
9b	-8.7	-8.8
9c	-8.7	-9.4
9d	-8.1	-6.8
9e	-7.5	-7.5
9f	-7.5	-8.0
9g	-8.0	-6.7
9h	-7.4	-9.1
9i	-7.5	-7.7
9j	-7.4	-7.4
9k	-7.4	-8.1
9l	-8.3	-6.7
9m	-7.3	-6.6
9n	-6.9	-7.7
9o	-8.2	-7.1
9p	-6.9	-8.2
9q	-7.4	-8.5
9r	-8.4	-5.5
9s	-7.7	-7.3
9t	-7.9	-7.8
Control (Celecoxib)	-9.3	-7.8

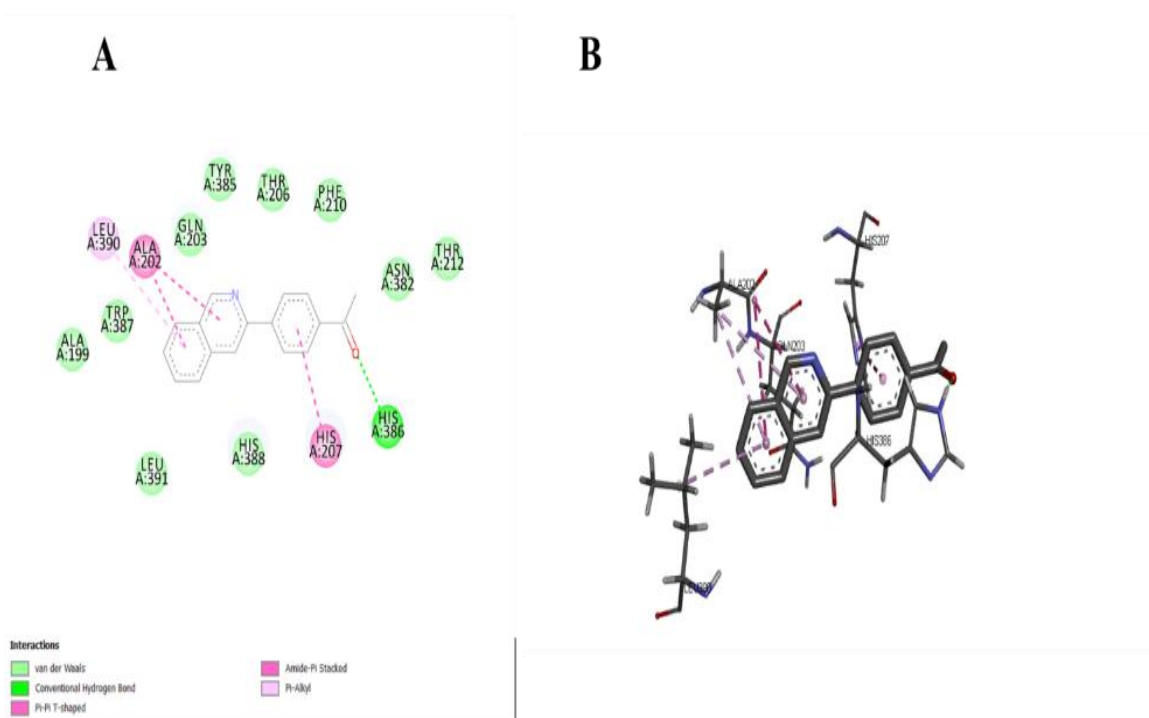


Figure 2. The binding interactions of protein 9a with the amino acid residues of COX-2's binding site are presented in 2D (A) and 3D (B) images (PDB ID: 5KIR).

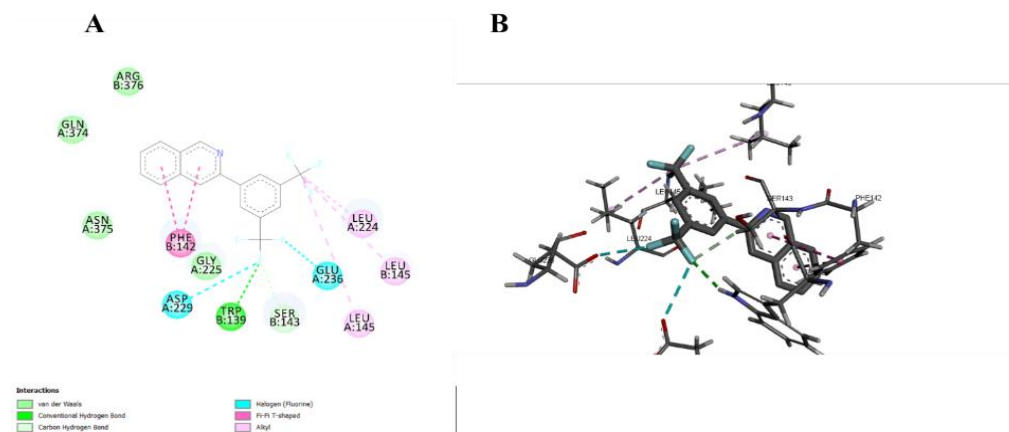


Figure 3. The binding interactions of protein 9b with the amino acid residues of COX-2's binding site are presented in 2D (A) and 3D (B) images (PDB ID: 5KIR).

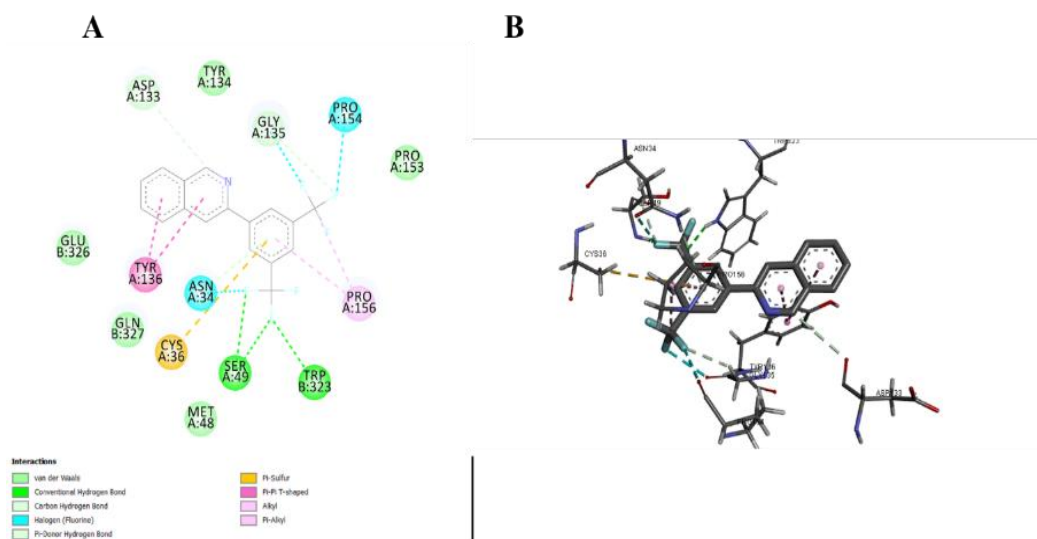


Figure 4. The binding interactions of protein 9c with the amino acid residues of COX-2's binding site are presented in 2D (A) and 3D (B) images (PDB ID: 5KIR).

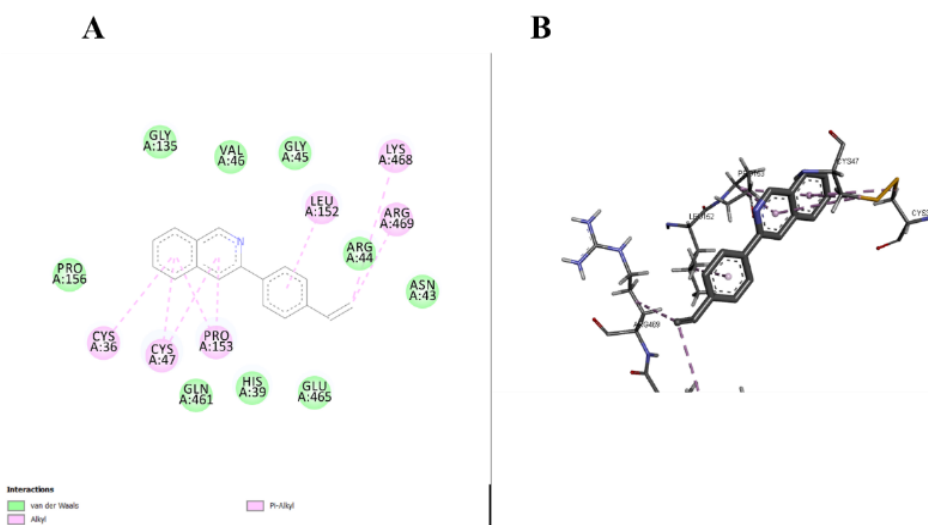


Figure 5. The binding interactions of protein 9l with the amino acid residues of COX-2's binding site are presented in 2D (A) and 3D (B) images (PDB ID: 5KIR).

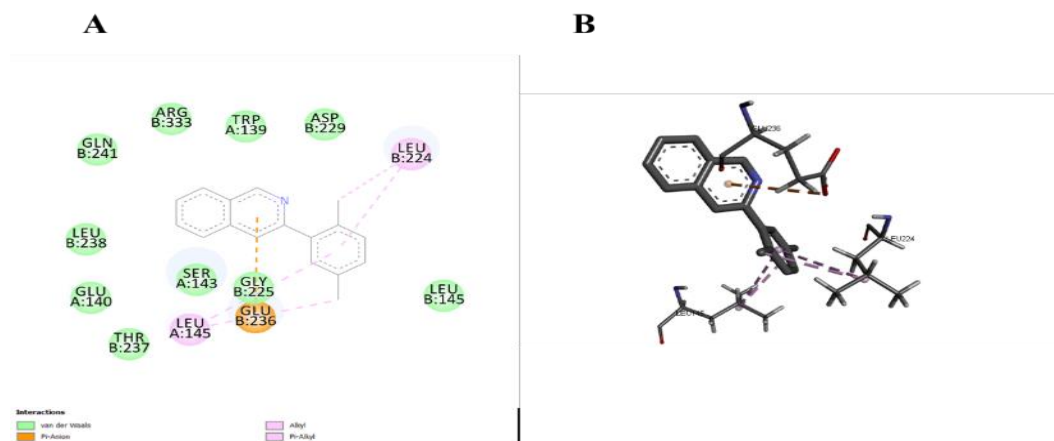


Figure 6. The binding interactions of protein 9q with the amino acid residues of COX-2's binding site are presented in 2D (A) and 3D (B) images (PDB ID: 5KIR).

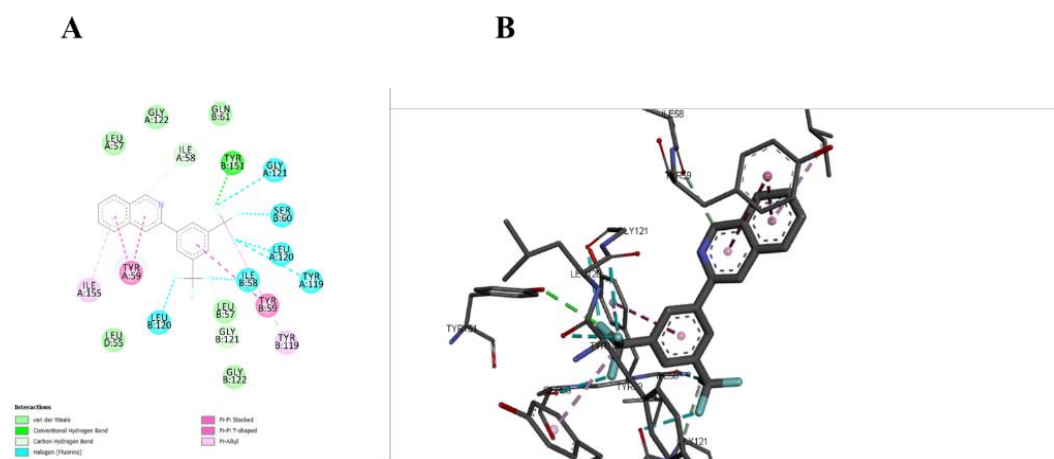


Figure 7. Presentation of the binding interactions of 9b with the TNF- binding site's amino acid residues in 2D(A) and 3D(B) space (PDB ID: 2AZ5).

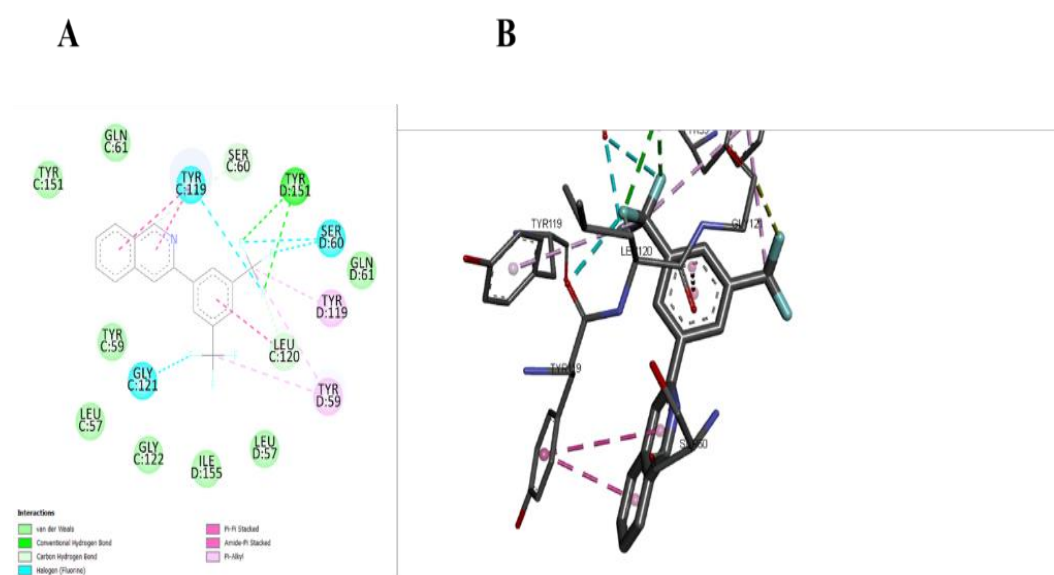


Figure 8. Presentation of the binding interactions of 9c with the TNF- binding site's amino acid residues in 2D(A) and 3D(B) space (PDB ID: 2AZ5).

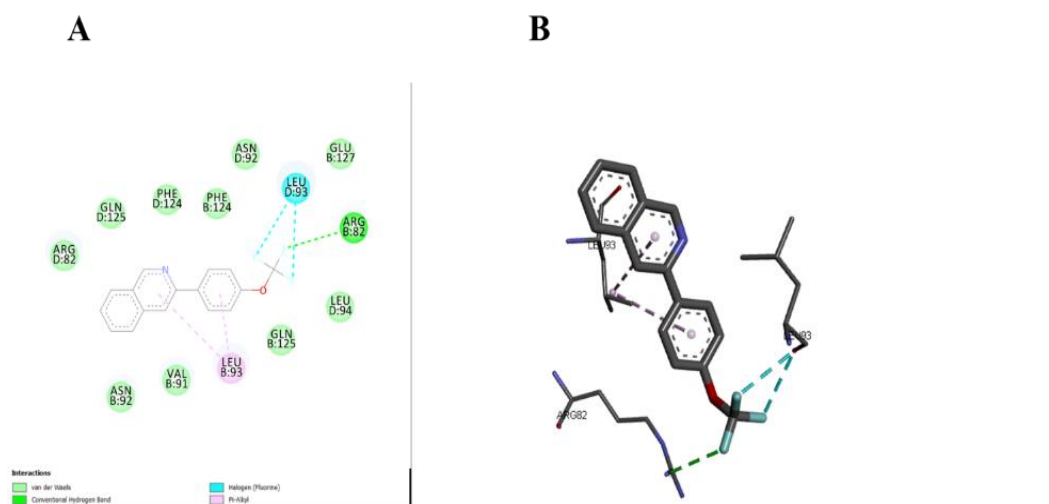


Figure 9. Presentation of the binding interactions of 9h with the TNF- binding site's amino acid residues in 2D(A) and 3D(B) space (PDB ID: 2AZ5).

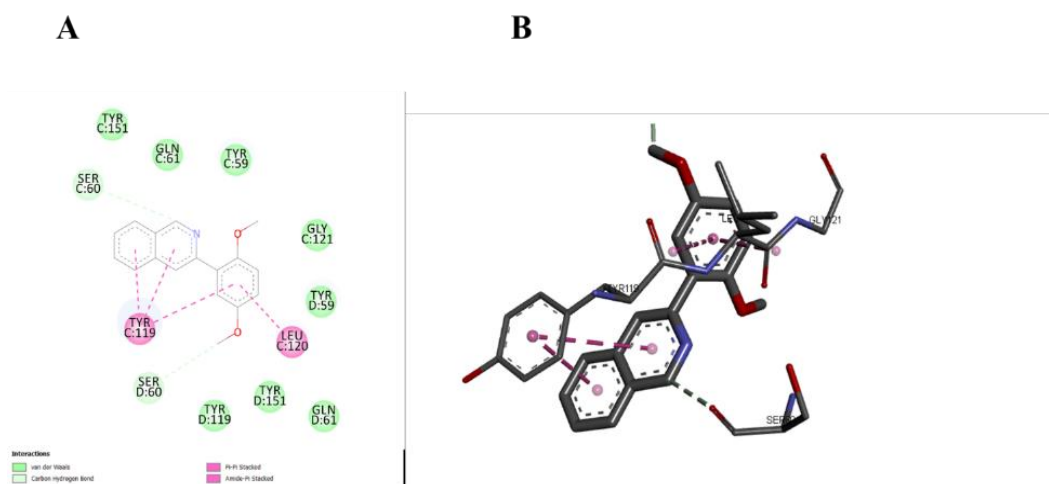


Figure 10. Presentation of the binding interactions of 9p with the TNF- binding site's amino acid residues in 2D(A) and 3D(B) space (PDB ID: 2AZ5).

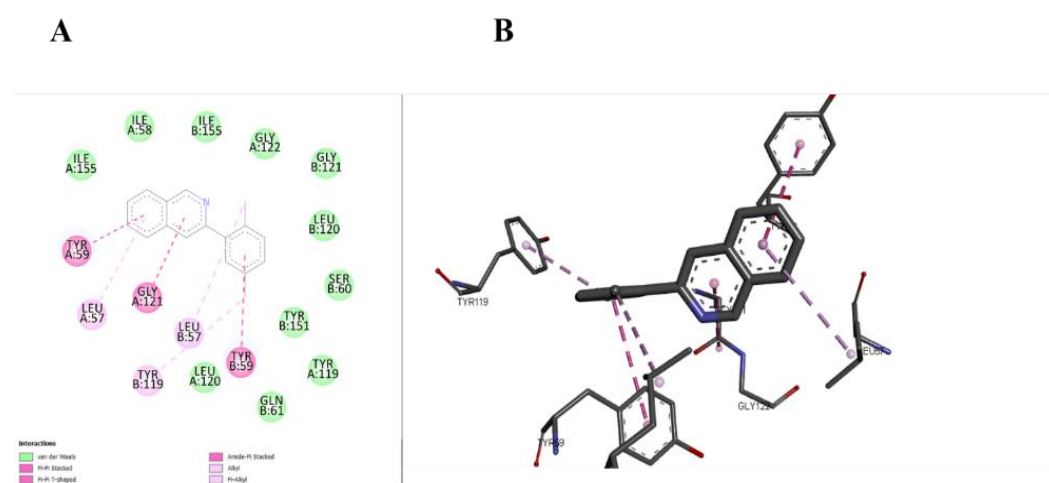


Figure 11. Presentation of the binding interactions of 9q with the TNF- binding site's amino acid residues in 2D(A) and 3D(B) space (PDB ID: 2AZ5).

2.5. Structural analysis of target proteins

COX-2 (PDB ID: 5KIR) has 1102 amino acids, 41% helices, 9% sheets, 98% positive phi and psi surface identity, and an R-value of 0.220. TNF- α (PDB ID: 2AZ5) has 542 amino acids, 66% alpha helix, 98% phi and psi surface positivity, and an R-value of 0.220. According to the Ramachandran plot, 98.00% of the amino acids for both target proteins fall within the acceptable phi (ϕ) and psi (ψ) angle limitations, as seen in Figure 14. This demonstrates that the amino acid conformation is quite good and structurally sound in both COX-2 and TNF- α . The Ramachandran plot shows that 98% of the phi (ϕ) and psi (ψ) angles are within the range predicted for stable protein structures, demonstrating good overall stability and protein folding.

2.6. Anti-Inflammatory activity

The activity of the tested compounds (9a, 9b, 9c, 9h, 9q), as well as reference standard, were measured via carrageenan-induced inflammation in albino rats. Rats (n = 6) were given an intraplantar injection of carrageenan (1%) and then the thickness of the paw was measured via plethysmometer after 3 hr. Carrageenan induced inflammation resulted in increased mean paw thickness in the negative control group. Among all compounds tested, 9b and 9q showed significant anti-inflammatory activity and reduced the mean paw thickness 3 hr. post carrageenan injection. Other compounds showed mild anti-inflammatory activity. These results, therefore, indicate that these newly synthesized nitrogen derivatives produce strong anti-inflammatory effects. Figure 12 depicts the results obtained.

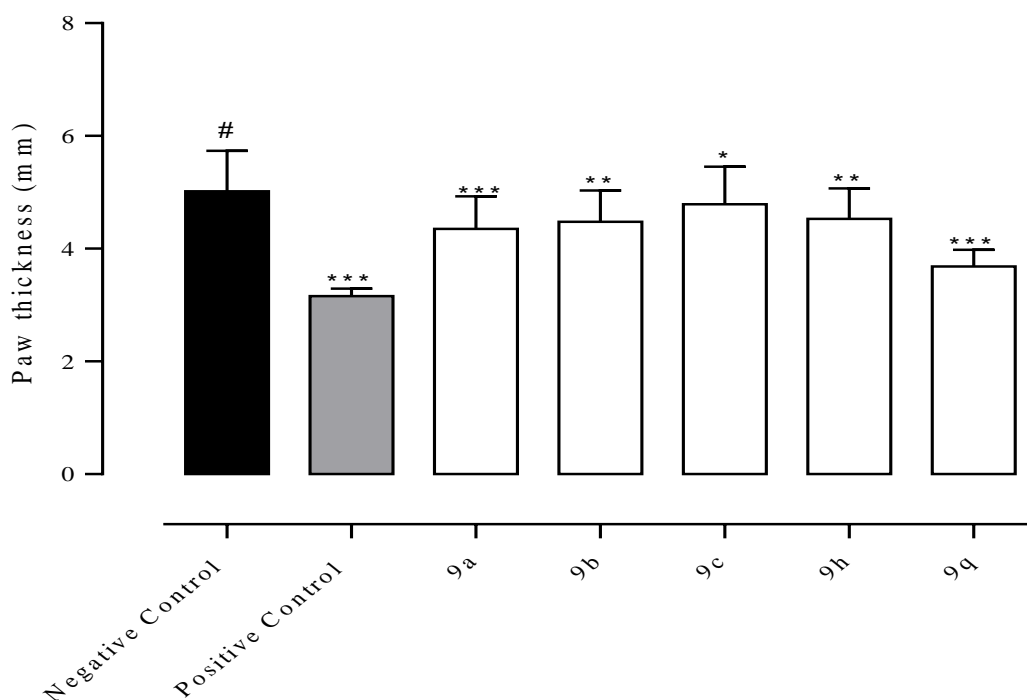


Figure 12. Effects of synthesized compounds on carrageenan-induced inflammation. The data was expressed as the mean \pm SEM, (n=6 / group). * p < 0.05, ** p < 0.01, *** p < 0.001 relative to negative control group, while #p < 0.05, is relative to saline control. Data is analyzed by one-way ANOVA followed by Turkey's multiple comparison test using GraphPad Prism (9.5.1) software.

2.7. Analgesic activity

The analgesic activity of the selected synthesized compounds (9a, 9b, 9c, 9h, 9q) was assessed by the hot plate method. According to the structure-activity relationship (SAR) studies, phenolic compounds have increased the analgesic activity, so most of the compounds exhibited analgesic

activity when compared with standard drug celecoxib. The analgesic activity of the compounds increased with time. 1 hr. after carrageenan injection, compound 9b and 9q significantly increased the latency time to heat stimuli and showed potent analgesic activity (Figure 13). The pretreatment with synthesized derivatives produced analgesic effects in the carrageenan-induced inflammatory pain model as indicated by the increase in latency time on hot plate.

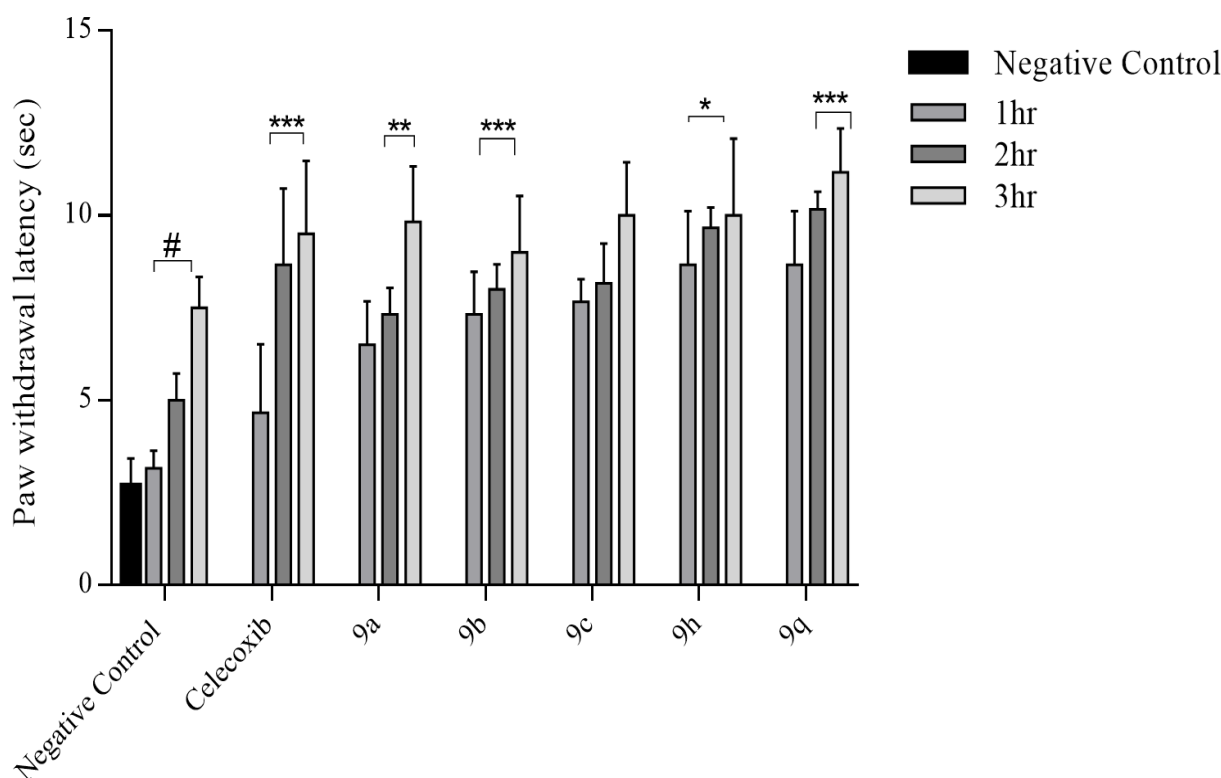


Figure 13. Effects of synthesized compounds on carrageenan-induced thermal hyperalgesia. The data was expressed as the mean \pm SEM, (n=6 / group). * $p < 0.05$, ** $p < 0.01$, *** $p < 0.001$ relative to negative control group, while # $p < 0.05$, is relative to saline control. Data is analyzed by one-way ANOVA followed by Turkey's multiple comparison test using GraphPad Prism (9.5.1) software.

Table 4. Animal body weight, water intake and food intake in treated and control animal groups.

Day	Group-A (Control)	Group-B (9a)	Group-C (9c)	Group-D (9h)
Animal Body Weight[40] (Mean \pm SD)				
Day 0 (Pre-Treated)	0.193 \pm 0.017	0.139 \pm 0.017	0.172 \pm 0.019	0.177 \pm 0.016
Day 1	0.197 \pm 0.017	0.142 \pm 0.017	0.174 \pm 0.018	0.179 \pm 0.019
Day 3	0.203 \pm 0.017	0.145 \pm 0.012	0.176 \pm 0.011	0.184 \pm 0.016
Day 5	0.209 \pm 0.018	0.145 \pm 0.015	0.178 \pm 0.015	0.187 \pm 0.015
Animal Water Intake (ml/animal/day) (Mean \pm SD)				
Day 1	30 \pm 0.01	35 \pm 0.015	35 \pm 0.012	30 \pm 0.01
Day 3	30 \pm 0.016	25 \pm 0.018	30 \pm 0.015	35 \pm 0.02
Day 5	31.5 \pm 0.019	35 \pm 0.011	32.5 \pm 0.010	36.5 \pm 0.017
Animal Food Intake (Kg/animal/day) (Mean \pm SD)				
Day 1	0.036 \pm 0.012	0.0125 \pm 0.011	0.0135 \pm 0.018	0.016 \pm 0.018
Day 3	0.050 \pm 0.10	0.0405 \pm 0.015	0.0105 \pm 0.014	0.024 \pm 0.020
Day 5	0.0295 \pm 0.016	0.0055 \pm 0.013	0.025 \pm 0.015	0.00375 \pm 0.021

Table 5: Animal Behavioral and mortality in treated and control animal groups.

Animal observation	Group-A (Control)	Group-B (9a)	Group-C (9c)	Group-D (9h)
Touch response	+	+	+	+
Corneal reflex	+	+	+	+
Alertness	+	+	+	+
Mortality	-	-	-	-
Signs of illness	-	-	-	-
Dermal toxicity	-	-	-	-
Ocular toxicity	-	-	-	-
Eye Irritation	-	-	-	-
Lacrimation	-	-	-	-
Hyperactivity	-	-	-	-

2.8. Acute oral Toxicity studies

Table 4, and Table 5 represent the effects of synthesized compounds on body weight, food body temperature, and water utilization, behavior pattern and toxicity associated symptoms in control group and treated groups. Treated animals displayed normal behavior pattern like control group. Animal feces were free of mucus or blood. The eating behavior of animals of control and treatment group was also normal. No mortality is seen in the treated groups. All rats were sensitive to stimulation, sound, and light. They had no salivation, no lacrimation, or running nose, dryness of mouth or edema.

3. Experimental Section

3.1. General Details

We used Analytical grade chemicals in the present work. All the chemicals and reagents were taken from renowned commercial sources (Merk®, Acros® and Alrich®). During experimental work chemicals were used without additional distillation and kept under nitrogen in airtight Schlenk tubes. During synthesis the solvents used were Ethyl acetate, methanol, n hexane, Chloroform, Dichloromethane, Acetone and Toluene. Moreover, all the solvents used were purified, saturated with nitrogen, and degassed before use.

We used Merck DC finished foils (silica gel 60 F₂₅₄ on aluminum) for thin layer chromatography (TLC), whereas for detection UV light with 254nm was used. Compact walled glass column over Merck silica gel 60 (0.063-0.200mm, 70-230 mesh) was used for column chromatography with ethyl acetate/n hexane mixture was used as eluting solvent both in TLC and column chromatography. Melting point of Compounds were taken in °C using melting point Gallenkamp capillary device and were noted on a digital melting point device, Stuart, SMP 10 (England).

Bruker-Advance 300 MHz spectrometer operating at Proton NMR 300 MHz with tetramethyl silane TMS as the internal standard was used to note NMR spectra. Tetramethylsilane was selected as reference with zero (0) ppm chemical shift value for measuring chemical shifts values of test compounds in ppm (δ -scale). Characterization of the signal fragmentations: s= singlet, d= doublet, t= triplet, m= multiplet dd= doublet of doublet, q= quartet and coupling constant (J- values) were mentioned in Hertz (Hz).

We used Thermo Scientific (NICOLET IS10) spectrophotometer for FTIR analysis (potassium bromide; KBr), (ν_{max} in cm^{-1}) along with an ANALYST 2000CHNS analyzer (Perkin Elmer) for analysis of the elements present. The physical data of the synthesized compounds is given in Table 2.

3.2. General Synthesis Procedure for arylated heterocyclic compounds

We chose Suzuki Miyaura coupling for our synthesis procedure keeping in mind its moderate reaction conditions, ease of synthesis and overall stability of the boronic acid derivatives, as well as the low toxicity of the resulting boron compounds and byproducts [41].

As illustrated in Scheme 1, 3-bromo isoquinoline (starting material) was treated with boronic acid for the synthesis of C–C coupling products via well-established Suzuki Miyaura coupling reaction(s) with slight modification. In the presence of base and catalyst the reaction temperature was kept within range (85-95 °C) for 8-9 hours. We monitored the reaction progress by TLC (Merck silica gel 60 F254) and after completion newly synthesized compounds were purified by using column chromatography. The suggested mechanism for the chemical reaction is presented in Scheme 2, with three main steps, i.e., oxidative addition, transmetallation and reductive elimination. The same reaction can also be carried out for synthesis of other cross-coupling reaction products by using different Boronic acids using same starting material [42].

3.2.1. 1-(4-(isoquinolin-3-yl) phenyl) ethanone (9a): Yellow crystalline solid, M.P. 239.75 °C; yield (78%), methanol/ethyl acetate /n-hexane (1:2:3). IR (KBr, cm⁻¹): 3029 (Ar-H), 2867(CH₂-stretching), 1680(C=O stretching), 1596 C=C coupled bond stretching, 1509 (C-C coupled bond stretching), 1213(C-N coupled bond stretching). ¹H NMR: δ 8.8 7.8 7.6 7.5 7.4 7.1 2.6. ¹³CNMR (CDCl₃, 100MHz) δ = 180 (C=O), 152(C-H), 150(C-H), 136(C-H), 131(C-H), 130(C-H), 128(C-H), 127(C-H), 126(C-H), 125(C-H), 21(O=C-CH₃), 19 (CH₃). UV visible 312 nm

3.2.2. 3-(2,4-bis(trifluoromethyl)phenyl) isoquinoline (9b): White crystalline solid, M.P. 210.52 °C; yield (71%), methanol/ethyl acetate /n-hexane (1:2:3). IR (KBr, cm⁻¹): 3047(Ar-H), 1604 C=C coupled bond stretching, 1508 (C-C coupled bond stretching), 1214(C-N coupled bond stretching). ¹H NMR: δ 8.9, 8.7, 8.4 8.0 7.6 7.5 7.4 7.1 2.6 2.4. ¹³CNMR (CDCl₃, 100MHz) δ = 152 (C-H), 150 (C-H), 136(C-H), 131(C-H), 130(C-H), 128(C-H), 127(C-H), 126(C-H), 125(C-H), 21(C-H), 19 (C-H). UV visible 275nm

3.2.3. 3-(4-fluoro-3-methylphenyl) isoquinoline (9c): Grey crystalline solid, M.P. 191.66 °C; yield (81%), methanol/ethyl acetate /n-hexane (1:2:3). IR (KBr, cm⁻¹): 3021(Ar-H), 2853 (CH₂-stretching), 1604 C=C coupled bond stretching, 1504 (C-C coupled bond stretching), 1216(C-N coupled bond stretching). ¹H NMR: δ 8.9, 8.7 8.0 7.6 7.5 7.4 7.1 2.6 2.4. ¹³CNMR (CDCl₃, 100MHz) δ = 152(C-H), 150(C-H), 136(C-H), 131(C-H), 130(C-H), 128(C-H), 127(C-H), 126(C-H), 125(C-H), 21(C-H), 19 (C-H). UV visible 318nm

3.2.4. 3-(4-(methylthio) phenyl) isoquinoline 9d: White crystalline solid, M.P. 212.95°C; yield (77%), Methanol/ethyl acetate /n-hexane (1:2:3). IR (KBr, cm⁻¹): 3025(Ar-H), 2840(CH₂-stretching), 1597 C=C coupled bond stretching, 1504 (C-C coupled bond stretching), 1208(C-N coupled bond stretching) ¹H NMR: δ 8.9(s, 1H), 8.1(s, 1H), 7.9(d, 1H, j= 7.4), 7.6(d, 2H, j= 7.4), 7.5(d, 2H, j= 7.4), 7.4(t, 2H, j= 7.4), 2.5 (s, 3H) . ¹³CNMR (CDCl₃, 100MHz) δ =152(C-H), 150(C-H), 136(C-H), 131(C-H), 130(C-H), 128(C-H), 127(C-H), 126(C-H), 125(C-H), 14(C-H). UV visible 382.2nm

3.2.5. 3-(2,3-dichlorophenyl) isoquinoline 9e: White crystalline solid, M.P. 239.64°C; yield (75%), methanol/ethyl acetate /n-hexane (1:2:3). IR (KBr, cm⁻¹): 3020(Ar-H), 2832(CH₂-stretching), 1604 C=C coupled bond stretching, 1509 (C-C coupled bond stretching), 1215(C-N coupled bond stretching). ¹H NMR: δ 8.9 8.1 7.6 7.5 7.4 7.1. ¹³CNMR (CDCl₃, 100MHz) δ =152(C-H), 150(C-H), 136(C-H), 131(C-H), 130(C-H), 128(C-H), 127(C-H), 126(C-H), 125(C-H). UV visible 290.2nm

3.2.6. 3-(4-phenoxyphenyl) isoquinoline 9f: White crystalline solid, M.P. 283.55°C; yield (67%), methanol/ethyl acetate /n-hexane (1:2:3). IR (KBr, cm⁻¹): 3015(Ar-H), 2845(CH₂-stretching), 1610 C=C coupled bond stretching, 1511 (C-C coupled bond stretching), 1221(C-N coupled bond stretching) ¹H NMR: δ 8.9 8.1 7.6 7.5 7.4 7.1. ¹³CNMR (CDCl₃, 100MHz) δ

=152(C-H), 150(C-H), 136(C-H), 131(C-H), 130(C-H), 128(C-H), 127(C-H), 126(C-H), 125(C-H), 36(C-H). UV visible 312.7nm

3.2.7. 3-(5-schorothiophen-2-yl) isoquinoline 9g: White crystalline solid, M.P. 260.87 °C; yield (69%), methanol/ethyl acetate /n-hexane (1:2:3). IR (KBr, cm^{-1}): 3015(Ar-H), 2848(CH₂-stretching), 1598 C=C coupled bond stretching, 1501 (C-C coupled bond stretching), 1201(C-N coupled bond stretching). ¹H NMR: δ 8.9 8.1 7.6 7.5 7.4 7.1. ¹³CNMR (CDCl₃, 100MHz) δ =152(C-H), 150(C-H), 136(C-H), 131(C-H), 130(C-H), 128(C-H), 127(C-H), 126(C-H), 125(C-H). UV visible 387.6nm

3.2.8. 3-(4-(trifluoromethoxy) phenyl) isoquinoline 9h: White crystalline solid, M.P. 204.97 °C; yield (69%), methanol/ethyl acetate /n-hexane (1:2:3). IR (KBr, cm^{-1}): 3038 (Ar-H), 1605 C=C coupled bond stretching, 1498 (C-C coupled bond stretching), 1218(C-N coupled bond stretching). 1125(R-OC coupled bond stretching). ¹H NMR: δ 8.9 8.0 7.6 7.5 7.4 7.1. ¹³CNMR (CDCl₃, 100MHz) δ =152(C-H), 150(C-H), 136(C-H), 131(C-H), 130(C-H), 128(C-H), 127(C-H), 126(C-H), 125(C-H), 21(C-H), 19 (C-H). UV visible 256 nm

3.2.9. 3-(3,5-difluorophenyl) isoquinoline 9i: White crystalline solid, M.P. 260.89°C; yield (83%), methanol/ethyl acetate /n-hexane (1:2:3). IR (KBr, cm^{-1}): 3010 (Ar-H), 2825(CH₂-stretching), 1595 C=C coupled bond stretching, 1512 (C-C coupled bond stretching), 1221(C-N coupled bond stretching). ¹H NMR: δ 8.9 8.1 7.6 7.5 7.4 7.1. ¹³CNMR (CDCl₃, 100MHz) δ =152(C-H), 150(C-H), 136(C-H), 131(C-H), 130(C-H), 128(C-H), 127(C-H), 126(C-H), 125(C-H). UV visible 275.7nm

3.2.10. 3-(2,4-difluorophenyl) isoquinoline 9j: White crystalline solid, M.P. 180.98°C; yield (82%), methanol/ethyl acetate /n-hexane (1:2:3). IR (KBr, cm^{-1}): 3012(Ar-H), 2835(CH₂-stretching), 1598 C=C coupled bond stretching, 1511 (C-C coupled bond stretching), 1221(C-N coupled bond stretching). ¹H NMR: δ 8.9 8.1 7.6 7.5 7.4 7.1. ¹³CNMR (CDCl₃, 100MHz) δ =152(C-H), 150(C-H), 136(C-H), 131(C-H), 130(C-H), 128(C-H), 127(C-H), 126(C-H), 125(C-H). UV visible 272.2nm

3.2.11. 3-(2,5-difluorophenyl) isoquinoline 9k: White crystalline solid, M.P. 261.18°C; yield (81%), methanol/ethyl acetate /n-hexane (1:2:3). IR (KBr, cm^{-1}): 3001(Ar-H), 2855(CH₂-stretching), 1599 C=C coupled bond stretching, 1511 (C-C coupled bond stretching), 1221(C-N coupled bond stretching). ¹H NMR: δ 8.9 8.1 7.6 7.5 7.4 7.1. ¹³CNMR (CDCl₃, 100MHz) δ =152(C-H), 150(C-H), 136(C-H), 131(C-H), 130(C-H), 128(C-H), 127(C-H), 126(C-H), 125(C-H). UV visible 276.3nm

3.2.12. 3-(4-vinylphenyl) isoquinoline 9l: White crystalline solid, M.P. 188.06°C; yield (76%), methanol/ethyl acetate /n-hexane (1:2:3). IR (KBr, cm^{-1}): 3011(Ar-H), 2835(CH₂- stretching), 1596 C=C coupled bond stretching, 1502 (C-C coupled bond stretching), 1230(C-N coupled bond stretching). ¹H NMR: δ 8.9 8.1 7.6 7.5 7.4 7.1 2.1 1.9. ¹³CNMR (CDCl₃, 100MHz) δ =152(C-H), 150(C-H), 136(C-H), 131(C-H), 130(C-H), 128(C-H), 127(C-H), 126(C-H), 125(C-H), 36(C-H), 32 (C-H). UV visible 232.1nm

3.2.13. 3-(furan-2-yl) isoquinoline 9m: White crystalline solid, M.P. 161.45°C; yield (71%), methanol/ethyl acetate /n-hexane (1:2:3). IR (KBr, cm^{-1}): 3013(Ar-H), 2855(CH₂- stretching), 1599 C=C coupled bond stretching, 1514 (C-C coupled bond stretching), 1208(C-N coupled bond stretching). ¹H NMR: δ 8.9 8.1 7.6 7.5 7.4 7.1. ¹³CNMR (CDCl₃, 100MHz) δ =152(C-H), 150(C-H), 136(C-H), 131(C-H), 130(C-H), 128(C-H), 127(C-H), 126(C-H), 125(C-H), 34(C-H). UV visible 332.7nm

3.2.14. 3-(3,4-dimethoxyphenyl) isoquinoline 9n: White crystalline solid, M.P. 246.8°C; yield (68%), methanol/ethyl acetate /n-hexane (1:2:3). IR (KBr, cm^{-1}): 3025(Ar-H), 2835(CH₂-stretching), 1605 C=C coupled bond stretching, 1513 (C-C coupled bond stretching), 1211(C-N coupled bond stretching). ¹H NMR: δ 8.9 8.1 7.6 7.5 7.4 7.1, 3.4. ¹³CNMR (CDCl₃, 100MHz) δ =152(C-H), 150(C-H), 136(C-H), 131(C-H), 130(C-H), 128(C-H), 127(C-H), 126(C-H), 125(C-H),36(C-H). UV visible 280.2nm

3.2.15. 3-(5bromo-2-methoxyphenyl) isoquinoline 9o: White crystalline solid, M.P. 273.1°C; yield (68%), methanol/ethyl acetate /n-hexane (1:2:3). IR (KBr, cm^{-1}): 3013(Ar-H), 2835(CH₂-stretching), 1599 C=C coupled bond stretching, 1515 (C-C coupled bond stretching), 1201(C-N coupled bond stretching). ¹H NMR: δ 8.9 8.1 7.6 7.5 7.4 7.1 3.4. ¹³CNMR (CDCl₃, 100MHz) δ =152(C-H), 150(C-H), 136(C-H), 131(C-H), 130(C-H), 128(C-H), 127(C-H), 126(C-H), 125(C-H), 34(C-H). UV visible 275.3nm

3.2.16. 3-(2,5-dimethoxyphenyl) isoquinoline 9p: White crystalline solid, M.P. 243.6°C; yield (74%), methanol/ethyl acetate /n-hexane (1:2:3). IR (KBr, cm^{-1}): 3016(Ar-H), 2845(CH₂-stretching), 1594 C=C coupled bond stretching, 1521 (C-C coupled bond stretching), 1209(C-N coupled bond stretching). ¹H NMR: δ 8.9 8.1 7.6 7.5 7.4 7.1 2.6 2.4. ¹³CNMR (CDCl₃, 100MHz) δ =152(C-H), 150(C-H), 136(C-H), 131(C-H), 130(C-H), 128(C-H), 127(C-H), 126(C-H), 125(C-H), 34(C-H). UV visible 269.7nm

3.2.17. 3-(2,5-dimethylphenyl) isoquinoline 9q: White crystalline solid, M.P. 202.34 °C; yield (76%), methanol/ethyl acetate /n-hexane (1:2:3). IR (KBr, cm^{-1}): 3010(Ar-H), 2825(CH₂-stretching), 1595 C=C coupled bond stretching, 1512 (C-C coupled bond stretching), 1221(C-N coupled bond stretching). ¹H NMR: δ 8.9 8.1 7.6 7.5 7.4 7.1 2.6 2.4. ¹³CNMR (CDCl₃, 100MHz) δ =152(C-H), 150(C-H), 136(C-H), 131(C-H), 130(C-H), 128(C-H), 127(C-H), 126(C-H), 125(C-H), 21(C-H), 19 (C-H). UV visible 275.7nm

3.2.18. 4-(isoquinolin-3-yl) phenol 9r: White crystalline solid, M.P. 266.48°C; yield (81%), methanol/ethyl acetate /n-hexane (1:2:3). IR (KBr, cm^{-1}): 3012(Ar-H), 2836(CH₂- stretching), 1594 C=C coupled bond stretching, 1511 (C-C coupled bond stretching), 1201(C-N coupled bond stretching). ¹H NMR: δ 8.9 8.1 7.6 7.5 7.4 7.1 3.2. ¹³CNMR (CDCl₃, 100MHz) δ =152(C-H), 150(C-H), 136(C-H), 131(C-H), 130(C-H), 128(C-H), 127(C-H), 126(C-H), 125(C-H), 34(C-H). UV visible 380.7nm

3.2.19. 3-(benzothiophen-2-yl) isoquinoline 9s: White crystalline solid, M.P. 308.73°C; yield (83%), methanol/ethyl acetate /n-hexane (1:2:3). IR (KBr, cm^{-1}): 3012(Ar-H), 2835(CH₂-stretching), 1593 C=C coupled bond stretching, 1511 (C-C coupled bond stretching), 1211(C-N coupled bond stretching). ¹H NMR: δ 8.9 8.1 7.6 7.5 7.4 7.1. ¹³CNMR (CDCl₃, 100MHz) δ =152(C-H), 150(C-H), 136(C-H), 131(C-H), 130(C-H), 128(C-H), 127(C-H), 126(C-H), 125(C-H), 34(C-H). UV visible 335nm

3.2.20. 3-phenylisoquinoline 9t: White crystalline solid, m.p 154.76°C; yield (85%), methanol/ethyl acetate /n-hexane (1:2:3). IR (KBr, cm^{-1}): 3010(Ar-H), 2835(CH₂- stretching), 1598 C=C coupled bond stretching, 1510 (C-C coupled bond stretching), 1221(C-N coupled bond stretching). ¹H NMR: δ 8.9 8.1 7.6 7.5 7.4 7.1. ¹³CNMR (CDCl₃, 100MHz) δ =152(C-H), 150 (C-H),136(C-H), 131(C-H), 130(C-H), 128(C-H), 127(C-H), 126(C-H), 125(C-H). UV visible 320.7nm

3.3. Molecular docking analysis of the Synthesized Compounds 9(a-t)

3.3.1. Retrieval of COX-2 and TNF- α structure from Protein Data Bank

Protein Data Bank (PDB) (www.rcsb.org) was used to access the three-dimensional (3D) structures of COX-2 and TNF- from Homo sapiens using the PDB IDs 5KIR and 2AZ5 respectively. Autodock Tools programme was used to prepare the target proteins for docking analysis. Moreover, proteins were reduced in energy, given Gasteiger charges and eventually saved in pdbqt format. Discovery Studio 4.1 Client (2012) produced hydrophobicity and Ramachandran graphs. VADAR was used to access the protein architecture and statistical percentage values of helices, -sheets, coils, and turns 1.8 [43].

3.2.2. Ligands-molecular docking

Discovery Studio Client was used to minimize the energy of the compounds and saved as ligand. The ligands were prepared utilising Autodock Tools in their most stable conformation after the addition of the Kolman and Gasteiger charges and kept in pdbqt format. The PyRx28 virtual screening tool run a molecular docking experiment for all the generated ligands against COX-2 and TNF-.with Auto Dock VINA Wizard approach [38] Grid box sizes (X = 86, Y = 126, Z = 126) and centre values (centre X = 48,321 centre Y = 19,448 centre Z = 33,145) for COX-2 were changed. For a better conformational position in the active region of the target protein, the grid box centre values for TNF- (centre X = -20.377, centre Y = 80.921, and centre Z = 50.33) and size values (X = 126, Y = 90, and Z = 124) were adjusted. Against COX-2 and TNF, ligands were docked separately with a default exhaustiveness value of 25. The lowest binding energy values (kcal/mol) were used to rank the predicted docked complexes. Discovery Studio (2.1.0) (Discovery Studio Visualizer Software, Version 4.0., 2012) produced the 3D graphical representations of all the docked complexes.

3.2.3. Structural analysis of target proteins

COX-2 (PDB ID: 5KIR) contained a total of 1102 amino acid residues and was made up of 41% helices (459 residues), 9% -sheets (102 residues), 49% coils (539 residues), 13% turns (144 residues), and 49% coils. The resolution was 2.70 and the R-value for the assigned protein appeared to be 0.220. The lengths were observed to have unit cell dimensions of a=126.989, b=149.422 and c=185.055 with 90° angle. The Ramachandran plot demonstrated that 98.00% of the amino acids dropped within the range of accepted phi (ϕ) and psi (ψ) angle ranges.

TNF- α (PDB ID: 2AZ5) had a total of 542 amino acid residues and was composed of up to 0% helices, 66% -sheets (358 residues), 33% coils (184 residues), 4% turns (24 residues), and 33% coils. The resolution was 2.10, and the R-value for the specified protein appeared to be 0.220. The lengths were observed to have unit cell dimensions of a=165.254, b=165.254, and c=63.728 with 90°, 120°, and 180° angles, respectively. 98% of the amino acids were in the permitted regions for the phi (ϕ) and psi (ψ) angles, according to the Ramachandran plot. Figure 14 illustrates the Ramachandran plots for the target proteins.

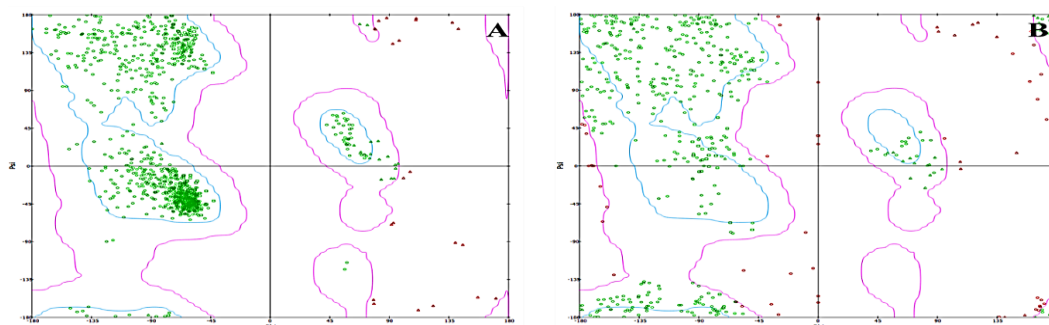


Figure 14. Ramachandran plots for target proteins, (A) COX-2 (PDB ID: 5KIR) and (B) TNF- α (PDB ID: 2AZ5).

3.4. *In vivo* pharmacological studies of synthesized compounds

3.4.1. *Induction of inflammatory pain and drug administration*

An experimental study was conducted on rats to induce acute inflammatory pain in the right hind paw by injecting 100 μ L of 1% carrageenan, after administering an intraperitoneal (IP) dose of drugs 30 minutes prior and compared with normal control group. Normal control group received normal saline injection into the paw whereas group of test animals received IP injections of 9a, 9b, 9c, 9h, and 9q (at a dose of 10 mg/kg), half an hour before the carrageenan injection. A negative control group received only an equal volume of vehicles (3% DMSO and 1.5% Tween-80), while the positive control group received celecoxib half an hour before the carrageenan injection.

3.4.2. *Thermal hyperalgesia*

To assess thermal hyperalgesia, a hot plate assay was conducted. Each animal was placed in a plexiglass chamber and positioned on a hot plate at 55 $^{\circ}$ C. The paw withdrawal latency was recorded using a stopwatch and all positive responses such as licking, flicking, or jumping were noted. A maximum cut-off time of 30 seconds was used to avoid tissue damage.

3.4.3. *Anti-inflammatory activity*

The anti-inflammatory activity of newly synthesized compounds were evaluated through the carrageenan-induced paw edema assay in rats, using celecoxib as a positive control.[44] Compounds 9a, 9b, 9c, 9h, and 9q were dissolved in 3% DMSO and 1.5% Tween-80. The rats were divided into groups (n=6) with a received dose of 10 mg/kg of the test compounds or 20 mg/kg of diclofenac. The control group received IP injection of 3% DMSO and 1.5% Tween-80 (5ml/kg). After 30 minutes of drug administration, edema was induced in the right hind paw of the rats by administering 100 μ L of carrageenan. The paw edema was measured using a plethysmometer before and 3 hours after carrageenan administration.

3.4.4. *Acute toxicity study*

For toxicity study 12 healthy adult albino rats of winstar strain (with weight approximately ranging from 250 g \pm 10) were obtained from the Animal house of the Faculty of Pharmacy at Capital University of Science and Technology (Fop-CUST), Islamabad. The rats were divided into four groups (n=3), with Group A serving as the control group. The other three groups, Group B, Group C and Group D were administered synthesized compounds 9a, 9c and 9h, respectively. In a preliminary experiment, no lethal dose or median lethal dose (LD50) was observed. Therefore, the maximum tolerance dose (MTD) was used to estimate the acute oral toxicity of the synthesized compounds. The rats were housed in a temperature-controlled room (25 \pm 2 $^{\circ}$ C), with a relative humidity of 65 \pm 5% and a 12-hour light/dark cycle. They were provided with a balanced diet and water. The control group received 1 ml/100 gm body weight of 0.9% saline orally, while the treatment groups were given a total dose of 100 mg/kg body weight of synthesized compounds. The animals were monitored for any changes in their behavior pattern. After 14 days, the rats were sacrificed by cervical dislocation, and blood samples were collected for hematology and biochemical blood analysis. Vital organs, including the heart, liver, spleen, kidney, stomach, and lung, were removed, washed, sliced, and stained with haematoxylin-eosin for histopathological examination. The study was approved by Research Ethics Committee (REC), FoP-CUST (REC/02/12/22).

Author Contributions: Funding acquisitions, study technique, resources, conception, and software development were all contributed to by the authors: T.J., H.U., S.A.R., M.T.K., N.S.M., A.S.S., N.G., A.R., A.I., H.J., A.R., and M.A.U.R The final version of the work has been published with the approval of all authors.

Acknowledgments: The authors are thankful to Dr. Muhammad Adeel, Institute of Chemical Sciences, Gomal University, D.I Khan, Pakistan; Dr. Nadeem Irshad, Pharmacy Department, Quaid-e-Azam University Islamabad, and Faculty of Pharmacy, Capital University of Science and Technology, Islamabad, Pakistan.

Conflicts of Interest: The authors declare no competing financial interest.

References

1. García-Ramírez, J., L.A. González-Cortés, and L.D. Miranda, *A Modular Synthesis of the Rhazinilam Family of Alkaloids and Analogs Thereof*. *Organic Letters*, 2022. **24**(44): p. 8093-8097.
2. Akhtar, J., et al., *Structure-activity relationship (SAR) study and design strategies of nitrogen-containing heterocyclic moieties for their anticancer activities*. *European journal of medicinal chemistry*, 2017. **125**: p. 143-189.
3. Heravi, M.M. and V. Zadsirjan, *Prescribed drugs containing nitrogen heterocycles: an overview*. *RSC advances*, 2020. **10**(72): p. 44247-44311.
4. Daidone, G., B. Maggio, and D. Schillaci, *Salicylanilide and its heterocyclic analogues. A comparative study of their antimicrobial activity*. *Pharmazie*, 1990. **45**(6): p. 441-442.
5. Almerico, A.M., et al., *Glycosidopyrroles Part 1. Acyclic derivatives: 1-(2-hydroxyethoxy) methylpyrroles as potential anti-viral agents*. *Il Farmaco*, 1998. **53**(1): p. 33-40.
6. Schaefer, E.J., et al., *Comparisons of effects of statins (atorvastatin, fluvastatin, lovastatin, pravastatin, and simvastatin) on fasting and postprandial lipoproteins in patients with coronary heart disease versus control subjects*. *The American journal of cardiology*, 2004. **93**(1): p. 31-39.
7. Balogun, S.K., et al., *Effects of Separate and Combined Chronic Ingestion of Codeine and Tramadol on Self Grooming Behavior of Male and Female Albino Rats*. *American Journal of Applied Psychology*, 2020. **9**(3): p. 66-76.
8. Liu, J.K. and W.T. Couldwell, *Intra-arterial papaverine infusions for the treatment of cerebral vasospasm induced by aneurysmal subarachnoid hemorrhage*. *Neurocritical care*, 2005. **2**: p. 124-132.
9. Neamati, N., et al., *Highly potent synthetic polyamides, bisdistamycins, and lexitropsins as inhibitors of human immunodeficiency virus type 1 integrase*. *Molecular Pharmacology*, 1998. **54**(2): p. 280-290.
10. Deidda, D., et al., *Bactericidal activities of the pyrrole derivative BM212 against multidrug-resistant and intramacrophagic Mycobacterium tuberculosis strains*. *Antimicrobial agents and chemotherapy*, 1998. **42**(11): p. 3035-3037.
11. Kikuchi, C., et al., *Tetrahydrobenzindoles: selective antagonists of the 5-HT7 receptor*. *Journal of medicinal chemistry*, 1999. **42**(4): p. 533-535.
12. Gujral, S.S., et al., *Suzuki cross coupling reaction-a review*. *Indo Glob. J. Pharm. Sci*, 2012. **2**: p. 351-367.
13. Hussain, I., J. Capricho, and M.A. Yawer, *Synthesis of Biaryls via Ligand-Free Suzuki-Miyaura Cross-Coupling Reactions: A Review of Homogeneous and Heterogeneous Catalytic Developments*. *Advanced Synthesis & Catalysis*, 2016. **358**(21): p. 3320-3349.

14. Wen, X., et al., *Privileged heterocycles for DNA-encoded library design and hit-to-lead optimization*. European Journal of Medicinal Chemistry, 2023: p. 115079.
15. Koperniku, A., *N-Silylated amines as valuable synthons in methods development toward pharmaceutically relevant small molecules*. 2019, University of British Columbia.
16. Kakhki, S., S. Shahosseini, and A. Zarghi, *Design and synthesis of pyrrolo [2, 1-a] isoquinoline-based derivatives as new cytotoxic agents*. Iranian Journal of Pharmaceutical Research: IJPR, 2016. **15**(4): p. 743.
17. Pashev, A.S., N.T. Burdzhiev, and E.R. Stanoeva, *Synthetic Approaches toward the Benzo [a] quinolizidine System. A Review*. Organic Preparations and Procedures International, 2016. **48**(6): p. 425-467.
18. Awuah, E. and A. Capretta, *Strategies and synthetic methods directed toward the preparation of libraries of substituted isoquinolines*. The Journal of Organic Chemistry, 2010. **75**(16): p. 5627-5634.
19. Zheng, B., et al., *Copper-catalyzed benign and efficient oxidation of tetrahydroisoquinolines and dihydroisoquinolines using air as a clean oxidant*. ACS omega, 2018. **3**(7): p. 8243-8252.
20. Pesarico, A.P., et al., *A novel isoquinoline compound abolishes chronic unpredictable mild stress-induced depressive-like behavior in mice*. Behavioural Brain Research, 2016. **307**: p. 73-83.
21. Yuan, H.-L., et al., *Diverse isoquinolines with anti-inflammatory and analgesic bioactivities from *Hypecoum erectum**. Journal of Ethnopharmacology, 2021. **270**: p. 113811.
22. Valipour, M., et al., *Dual action anti-inflammatory/antiviral isoquinoline alkaloids as potent naturally occurring anti-SARS-CoV-2 agents: A combined pharmacological and medicinal chemistry perspective*. Phytotherapy Research, 2023.
23. Springob, K. and T.M. Kutchan, *Introduction to the different classes of natural products*. Plant-derived natural products: Synthesis, function, and application, 2009: p. 3-50.
24. Mäder, P. and L. Kattner, *Sulfoximines as rising stars in modern drug discovery? Current status and perspective on an emerging functional group in medicinal chemistry*. Journal of Medicinal Chemistry, 2020. **63**(23): p. 14243-14275.
25. Hosseinzadeh, Z., A. Ramazani, and N. Razzaghi-Asl, *Anti-cancer nitrogen-containing heterocyclic compounds*. Current Organic Chemistry, 2018. **22**(23): p. 2256-2279.
26. Le, M., *Applications of Sodium Azide in the Synthesis of Tetrazines and Hydrolysis Reactions*. 2021.
27. Gaybullayevna, S.G., *SYNTHESIS OF DRUGS FROM NITROGEN HETEROCYCLIC COMPOUNDS*. Новости образования: исследование в XXI веке, 2022. **1**(5): p. 945-955.
28. Amin, A., et al., *A Review on The Medicinal And Industrial Applications of N-Containing Heterocycles*. The Open Medicinal Chemistry Journal, 2022. **16**(1).
29. Vitaku, E., D.T. Smith, and J.T. Njardarson, *Analysis of the structural diversity, substitution patterns, and frequency of nitrogen heterocycles among US FDA approved pharmaceuticals: miniperspective*. Journal of medicinal chemistry, 2014. **57**(24): p. 10257-10274.
30. Heravi, M.M. and B. Talaei, *Ketenes as privileged synthons in the synthesis of heterocyclic compounds part 3: six-membered heterocycles*, in *Advances in Heterocyclic Chemistry*. 2016, Elsevier. p. 195-291.

31. Elrayess, R., et al., *Quinoline–hydrazone hybrids as dual mutant EGFR inhibitors with promising metallic nanoparticle loading: rationalized design, synthesis, biological investigation and computational studies*. New Journal of Chemistry, 2022. **46**(38): p. 18207-18232.
32. Henary, M., et al., *Benefits and applications of microwave-assisted synthesis of nitrogen containing heterocycles in medicinal chemistry*. RSC advances, 2020. **10**(24): p. 14170-14197.
33. Gatadi, S., T.V. Lakshmi, and S. Nanduri, *4 (3H)-Quinazolinone derivatives: Promising antibacterial drug leads*. European journal of medicinal chemistry, 2019. **170**: p. 157-172.
34. Zarenezhad, E., M. Farjam, and A. Iraj, *Synthesis and biological activity of pyrimidines-containing hybrids: Focusing on pharmacological application*. Journal of Molecular Structure, 2021. **1230**: p. 129833.
35. Borah, P., et al., *Heterocyclic compounds as antimicrobial agents*, in *Viral, Parasitic, Bacterial, and Fungal Infections*. 2023, Elsevier. p. 781-804.
36. Gao, F., et al., *Synthesis and biological evaluation of novel sinomenine derivatives as anti-inflammatory and analgesic agent*. RSC advances, 2022. **12**(46): p. 30001-30007.
37. Nicolaou, K.e.C., S.P. Ellery, and J.S. Chen, *Samarium diiodide mediated reactions in total synthesis*. Angewandte Chemie International Edition, 2009. **48**(39): p. 7140-7165.
38. Trott, O. and A.J. Olson, *AutoDock Vina: improving the speed and accuracy of docking with a new scoring function, efficient optimization, and multithreading*. J. Comput. Chem., 2010. **31**(2): p. 455-461.
39. Dallakyan, S. and A.J. Olson, *Small-molecule library screening by docking with PyRx*, in *Chem. Biol.* 2015, Springer. p. 243-250.
40. Anandarajagopal, K., et al., *2-Mercaptobenzimidazole derivatives: synthesis and anticonvulsant activity*. Advances in Applied Science Research, 2010. **1**(2): p. 132-138.
41. He, Z., et al., *Transition-metal-free Suzuki-type cross-coupling reaction of benzyl halides and boronic acids via 1, 2-metalate shift*. Journal of the American Chemical Society, 2018. **140**(7): p. 2693-2699.
42. Khan, I., et al., *Palladium-catalyzed synthesis of pyrimidine substituted diaryl ethers through Suzuki Miyaura coupling reactions: Experimental and DFT studies*. Optik, 2020. **219**: p. 165285.
43. Willard, L., et al., *VADAR: a web server for quantitative evaluation of protein structure quality*. Nucleic Acids Res., 2003. **31**(13): p. 3316-3319.
44. Khan, S., et al., *Studies on anti-inflammatory and analgesic activities of betel nut in rodents*. Journal of Ethnopharmacology, 2011. **135**(3): p. 654-661.